Nano Research
DOI 10.1007/s12274-015-0959-8
Research Article
ISSN 1998-0124
CN 11-5974/O4

Theoretical study on two-dimensional MoS_2 piezoelectric nanogenerators

Yongli Zhou[1,§], Wei Liu[1,§] (✉), Xin Huang[1,§], Aihua Zhang[1], Yan Zhang[2], and Zhong Lin Wang[1,3] (✉)

[1] *Beijing Institute of Nanoenergy and Nanosystems, Chinese Academy of Sciences, Beijing 100083, China*
[2] *Institute of Theoretical Physics, and Key Laboratory for Magnetism and Magnetic Materials of MOE, Lanzhou University, Lanzhou 730000, China*
[3] *School of Materials Science and Engineering, Georgia Institute of Technology, Atlanta, GA 30332, USA*
[§] *These authors contributed equally to this work.*

Received: 29 September 2015
Revised: 20 November 2015
Accepted: 25 November 2015

KEYWORDS
piezoelectric nanogenerator, MoS_2, two-dimensional, mechanical-electrical energy conversion, high-frequency application

ABSTRACT

Recent experiments have demonstrated that nanogenerators fabricated using two-dimensional MoS_2 flakes may find potential applications in electromechanical sensing, wearable technology, pervasive computing, and implanted devices. In the present study, we theoretically examined the effect of the number of atomic layers in MoS_2 flakes on the nanogenerator output. Under a square-wave applied strain, MoS_2 flakes with an even number of atomic layers did not exhibit a piezoelectric output, owing to the presence of a projected inversion symmetry. On the other hand, for MoS_2 flakes with an odd number of layers, owing to the lack of inversion symmetry, piezoelectric output voltage and current were generated, and decreased with the increase of the number of layers. Furthermore, as MoS_2 flakes were only a few atoms thick, the capacitance of the MoS_2 nanogenerators was at least an order of magnitude smaller than that of the nanowire- and nanofilm-based nanogenerators, enabling the use of MoS_2 nanogenerators in high-frequency applications. Our results explain the experimental observations and provide guidance on optimizing and designing two-dimensional nanogenerators.

1 Introduction

Mechanical energy in its different forms—including air flow and vibration, hydraulic pressure, and body movements—is widely present in the ambient environment, pervading our everyday life, and can be utilized to supplement the world energy demands. Piezoelectric semiconductors, such as wurtzite-structured ZnO [1–3], GaN [4–6], and InN [7, 8], possess coupled piezoelectric and semiconductor properties, and can be used to fabricate piezoelectric nanogenerators (NGs), which convert mechanical energy into electricity [9]. Under an external applied strain, piezoelectric semiconductor nanowires, or

Address correspondence to Wei Liu, wliu@binn.cas.cn; Zhong Lin Wang, zlwang@gatech.edu

nanofilms, can generate a piezoelectric potential, and strain-induced piezoelectric charges (piezocharges) at the nanowire, or nanofilm, edges can drive the flow of electrons through an external circuit. When the applied strain is released, the electrons flow back in the opposite direction. Until now, NGs with different structures have been developed, such as thin-film based NGs [10], vertical or lateral nanowire array integrated NGs [11], and two-dimensional (2D) woven NGs [12], in the attempt to achieve industrial production and scalable applications.

Recently, piezoelectricity and piezotronic effect have been observed in 2D atomic-thin MoS_2 flakes for the first time [13]. Compared with the early fabricated nanowire- and nanofilm-based NGs, MoS_2 NGs have the advantage of withstanding enormous strains (up to 17% [14]). Furthermore, MoS_2-based power cells can be integrated with graphene and other 2D functional units or devices to construct an atomic-thin self-powered nanosystem that can operate without external bias by harvesting energy from the ambient environment. However, it has been experimentally found that the piezoelectric output of MoS_2 NGs is sensitive to the number of atomic layers in the MoS_2 flakes [13]. In the case of even-layer flakes, almost no output is detected; on the other hand, for odd-layer flakes, the piezoelectric output can be observed, but decreases with the number of layers. The above observation requires further theoretical investigation.

In this study, we theoretically examined the output performance of MoS_2 NGs including up to seven atomic layers of MoS_2. Even-layer NGs exhibited almost no output, which could be attributed to the presence of a projected inversion symmetry in the MoS_2 flakes. On the contrary, owing to the absence of inversion symmetry, odd-layer NGs showed a clear signal, which decreased with the increase of the number of layers because of the rising capacitance. Furthermore, as the thickness of the MoS_2 NGs lies in the nanoscale region, their capacitance is at least an order of magnitude smaller than that of nanowire- and nanofilm-based NGs, enabling the potential application of MoS_2 NGs in high-frequency functional devices. This study provides a deeper understanding of the performance of 2D NGs, offering accurate guidance for future device design.

2 Model and method

Figure 1(a) shows a typical structure of a MoS_2 NG. In this model, a MoS_2 flake consisting of three atomic layers is sandwiched between the left-hand and right-hand electrodes. Each MoS_2 layer is parallel to the x–y plane. MoS_2 layers are numbered from bottom to top along the z-axis. For MoS_2 layers with an odd number, the $(\bar{1}010)$ zigzag edge (terminated by S atoms) is in contact with the left electrode, while the $(10\bar{1}0)$ zigzag edge (terminated by Mo atoms) is in contact with the right electrode. On the other hand, MoS_2 layers with an even number have an inverse orientation to the adjacent layers [15]: The $(\bar{1}010)$ edge is in contact with the right electrode, while the $(10\bar{1}0)$ edge is in contact with the left electrode. R_{Ex} is an external load resistor, which is connected to the two electrodes. MoS_2 NGs with a different number of layers can be similarly modeled by using the above method. According to the symmetry analysis, single-layer MoS_2 has only one non-zero independent piezoelectric constant, e_{11} [13]. Thus, in the present study, the external strains were applied along the x-axis, which led to a piezoelectric polarization along the same direction. To reveal the intrinsic properties of the MoS_2 NG, we adopted a simple resistor-capacitor (RC) circuit to describe the NG electrical characteristics. According to previous experimental and theoretical analyses [13, 16], MoS_2 NGs have three components: R_{In} is the NG internal resistance, C_{NG} is the NG capacitance, and V is the voltage source, which utilizes the piezopotential to drive the electron flow through the circuit. The equivalent circuit of the MoS_2 NG with R_{Ex} is shown in Fig. 1(b).

The static electrical characteristics of the MoS_2 NG, including the open-circuit voltage V, the surface

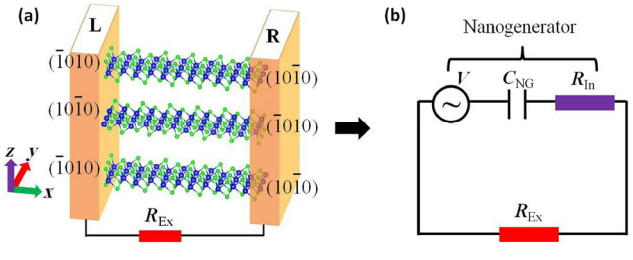

Figure 1 (a) Schematic illustration of a three-layer MoS_2 NG in connection with an external load resistor R_{Ex}. (b) Equivalent circuit of the three-layer MoS_2 NG.

piezocharge Q at the zigzag edge under an external applied strain, and C_{NG}, were numerically simulated by the COMSOL software package following the method adopted in the previous study [16]. Here, V was equal to the piezoelectric potential difference between the two electrodes; Q at the two zigzag edges was calculated as the negative of the artificially added charges that canceled the piezopotential, resulting in a zero potential difference between the two electrodes. In most simulations, the MoS_2 flake had a length (along the x-axis) of 50 nm, width (along the y-axis) of 50 nm, and thickness of $n \times 0.65$ nm, where n is the number of atomic layers in the flake and 0.65 nm is the thickness of a single MoS_2 layer [13]. To explore the dependence of the single-layer NG output on its in-plane dimensions, MoS_2 flakes with different lengths and widths, ranging from 10 to 300 nm, were also simulated (refer to section 3.1). Compared with the MoS_2 flakes used in the previous experiment, which had an in-plane size of 5 μm × 5 μm [13], the flakes used in the present study were quite small because of the convergence difficulties of the COMSOL program when simulating slab materials with a length/thickness ratio larger than 100. Indeed, single-layer MoS_2 flakes with an in-plane size of 5 nm × 5 nm can be experimentally fabricated [17]; thus, we believe that the MoS_2 NGs simulated in the present study could be realized in future experiments. For single-layer MoS_2, the adopted relative dielectric constant was ε_r = 3.3, the Poisson ratio v = 0.34, the elastic constants C_1 = 200 GPa and C_{12} = 49 GPa, and the piezoelectric constant e_{11} = 0.45 C·m^{-2} [18, 19]. To examine the dynamical properties of the MoS_2 NG in the circuit, a square-wave strain (refer to Fig. 3(a) in section 3.2) was applied, following the previous experiment [13]. The time-dependent short-circuit current, $I_{sq}(t)$, and output current in the external circuit were calculated as follows: (1) First, the time-dependent voltage $V(t)$ of the voltage source (refer to Fig. 1(b)) was obtained as V of the NG under real-time applied strain; (2) the time-dependent current $I(t)$ was calculated, using $V(t)$, by the PSpice program. In the circuit simulation, the adopted C_{NG} of the MoS_2 NG was numerically calculated by the COMSOL program, as mentioned above. The adopted NG R_{In}, which was obtained as V divided by the maximum $I_{sq}(t)$ in the previous experiment, was equal to 800 MΩ [13].

3 Results and discussion

3.1 Static behavior of MoS_2 NGs

First, we focused on the static properties of a single-layer MoS_2 NG. As the MoS_2 NG has a 2D atomic-thin structure, the previously used parallel capacitor model was not suitable for describing the current system, and the analysis of the NG V, Q, and C_{NG} had to be based on the relation $dV = dQ/C$. Figure 2(a) shows the linear dependence of V and Q density at the MoS_2-right electrode interface (MoS_2 $10\bar{1}0$ edge), which is obtained as Q divided by the MoS_2 edge area, under the applied strain. Under a tensile strain, positive piezocharges were created at the MoS_2 right electrode interface, and equivalent negative piezocharges were created at the MoS_2 left electrode interface; thus, the single-layer MoS_2 NG had positive V values (the electrical potential at the right electrode was higher than that at the left electrode). The above simulation results were consistent with previous studies [13, 20]. Figure 2(b) shows the dependence of V and Q density on the MoS_2 flake length for a single-layer NG under an applied tensile strain of 0.5%. As the flake length increased, the V values of the NG increased until saturation at ~200 nm, whereas the Q density retained almost the same value. In addition, both V and Q density did not depend on the flake width. The saturation of the NG V deviated from the previous theoretical results obtained for the nanowire- and nanofilm-based NGs, in which V was linearly dependent on the nanowire length or film thickness [10, 21], indicating that the previously adopted parallel capacitor model was not appropriate for describing the static behavior of the 2D NGs, and a numerical simulation for accurate capacitance was necessary. On the other hand, the Q density is an intrinsic property of MoS_2, which was determined by the applied strain and did not depend on the flake length.

As V of the single-layer NG saturated at the length of 200 nm and did not depend on the flake width, we could estimate V of an experimentally used 5 μm × 5 μm NG as equal to ~0.35 V, which was considerably larger than the value of 15 mV observed under a 0.5% strain [13]. The large difference between calculation and experimental results may be due to three main

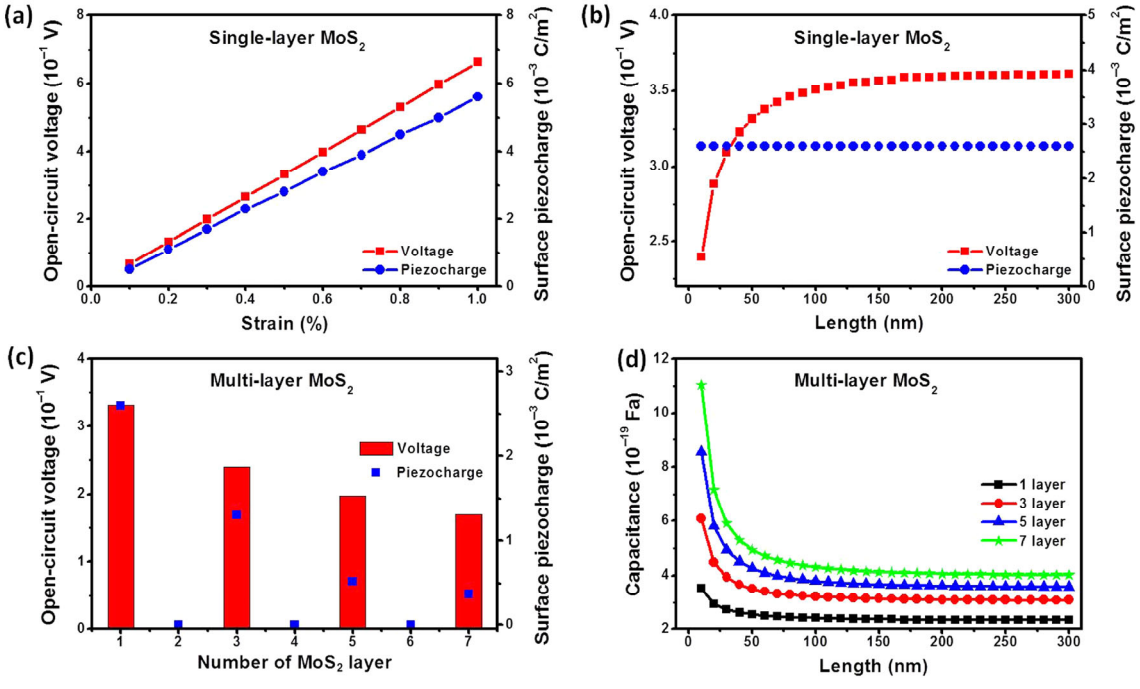

Figure 2 (a) Open-circuit voltage and surface piezocharge density of a single-layer MoS_2 NG are linearly dependent on the applied tensile strain. (b) Open-circuit voltage and surface piezocharge density of a single-layer MoS_2 NG versus MoS_2 flake length under a 0.5% applied tensile strain. (c) Influence of the MoS_2 layer number n on the NG open-circuit voltage and surface piezocharge under a 0.5% tensile strain. (d) Dependence of the odd-layer NG capacitance on the flake length.

factors: (1) In the experiment, the large C_{NG} of the NG may rise because of the two electrode plates, thus decreasing V; (2) the strain-induced piezocharges may be partially screened by free carriers in MoS_2 [13]; (3) according to the previous studies [17, 20], localized metallic states exist at the edge of the MoS_2 flake, which can be eliminated by contacting the metal electrode. At the NG interface, however, different types of defects may appear, such as vacancies or dislocations, which may break the bonding between MoS_2 and the metal electrode, thus resulting in the screening of the piezoelectric output by the localized metallic states. To enhance the piezoelectric output of the MoS_2 NG in future experiments, the optimization of the NG structure to minimize the electrode capacitance and eliminate the free carriers and edge metallic states in the MoS_2 surface is required.

Next, we discuss the variation of the NG piezoelectric output with the number of MoS_2 layers. By adopting an external tensile strain of 0.5%, as shown in Fig. 2(c), V and Q density exhibited a similar behavior, which was dependent on the layer number: For the NGs with an even number of MoS_2 layers, owing to the existence of the inversion symmetry, V and Q density were almost zero, indicating no piezoelectric output from these NGs; on the other hand, for the NGs with an odd number of atomic layers, the inversion symmetry was broken because of the unpaired single-layer MoS_2, resulting in evident V and Q. In the case of the odd-layer NG, the total Q did not change by increasing the layer number in the MoS_2 flake, as all the piezocharges were provided by the unpaired single-layer MoS_2. Hence, the Q density was inversely proportional to the layer number as a consequence of the enlargement of the edge surface area in NGs with more MoS_2 layers. Furthermore, C_{NG} increased with the number of layers, as shown in Fig. 2(d), which led to the decrease of V. Figure 2(d) also shows the length dependence of C_{NG}; the saturation of C_{NG} from a length of 200 nm can be observed. The saturation of C_{NG} resulted in the saturation of V, as shown in Fig. 2(b). From Fig. 2(d), we can estimate the capacitance of a 50 nm × 50 nm single-layer MoS_2 flake as 2.55×10^{-19} F, which is close to the experimentally measured value [22]. As a comparison, the capacitance of a fabricated ZnO nanowire, which typically has a diameter of 2 μm and a length

of 200 μm [2, 23], is at least one order of magnitude larger than that of the MoS_2 NG. The smaller C_{NG} of the MoS_2 NG, which derives from its atomic scale thickness, is an advantage in harvesting high-frequency mechanical signals.

3.2 Dynamic output of MoS_2 NG under square-wave applied strain

After discussing the static behavior of the MoS_2 NG, the dynamical output of the MoS_2 NG is examined in the present section. Figure 3(a) shows the square-wave applied strain used in the simulation. To emphasize the ability of the MoS_2 NG in harvesting high-frequency mechanical signals, we adopted a periodical strain with a frequency of 0.5 GHz, namely, the periodicity of the strain was only 2 ns. Figure 3(b) shows the $I_{sq}(t)$ values (setting the R_{Ex} in Fig. 1(b) equal to zero) of NGs with different numbers of MoS_2 layers. Figures 3(a) and 3(b) show two cycles of energy harvesting and conversion from the mechanical to the electrical domain. For the first circle, at time t = 4 ns in Fig. 3(a), a 0.5% tensile strain is suddenly applied on the NG. Effective piezocharges were induced at the zigzag edges of the MoS_2 flake, driving the electron flow from the left electrode to the right electrode in the external circuit and giving rise to a current peak at around the same time. As the time elapsed, the electrons accumulated at the interfacial region between the right electrode and MoS_2; the effect of the piezocharges was balanced by the accumulated electrons, and the current gradually decreased to zero. When the tensile strain was released at t = 5 ns, the piezocharges vanished immediately, and the electrons previously accumulated in the interfacial region flowed back from the right electrode to the left electrode through the external circuit, returning the system to the original state and leading to a negative current flow during the time period between 5 and 6 ns. As the equivalent circuit of the MoS_2 NG is an RC-circuit, the decrease of $I_{sq}(t)$ from the peak value to zero could be understood by considering the capacitor discharging. Within each half cycle (e.g., t = ~4–5 ns in Fig. 3(b)), $I_{sq}(t)$ followed the equation: $I_{sq}(t) = I_0(t_0)e^{\frac{-(t-t_0)}{R_{In}C_{NG}}}$. In the equation, $t_0 \leqslant t$ is the time when the tensile strain is applied on, or released from, the MoS_2 NG (refer to t = 4, 5, 6, and 7 ns in Fig. 3(b)), and $I_0(t_0) = V(t_0)/R_{In}$ is the maximum current at the time $t = t_0$. The above equation suggests that the time-dependent $I_{sq}(t)$ followed an exponential decay after the strain was applied on, or released from, the NG, which was consistent with the experimental results [13]. The RC time constant of the circuit, which is the time required for the current to fall to 1/e, was equal to $R_{In}C_{NG}$. Providing the same R_{In}, in the present study, the RC constants were larger for those NGs with a higher number of MoS_2 layers, resulting in the slower decay rate of $I_{sq}(t)$, as shown in Fig. 3(b).

Notably, in the current work, the output time of the MoS_2 NG was in the nanosecond scale, which is drastically smaller than the time scale observed in the previous experiment [13]. As mentioned in the previous section, the high-frequency application of the MoS_2 NG is due to its small C_{NG}, which is a consequence of the atomic-scale thickness of the MoS_2 flake. On the

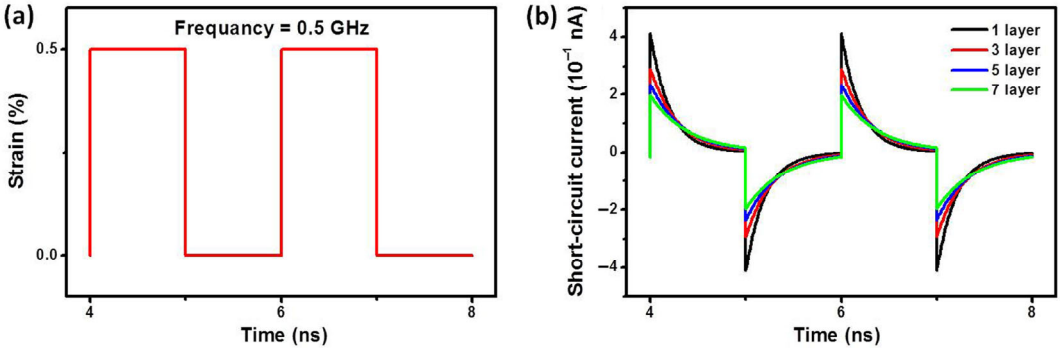

Figure 3 (a) Square-wave external strain applied on and released from the NG. (b) Corresponding short-circuit currents of odd-layer MoS_2 NGs under applied strain. Both figures show two cycles of energy harvesting and conversion from the mechanical to the electrical domain by the MoS_2 NGs.

other hand, in the MoS_2 NG experiment, the large time scale of the NG output was originated from the large capacitance in the circuit, which may be due to the parallel connection of the capacitance from the electrode plates. By optimizing the NG circuit and improving the fabrication techniques, we believe that MoS_2 NGs with high-frequency output can be realized in future.

Under the same square-wave applied strain with a tensile strain of 0.5% (Fig. 3(a)), the dynamical response of MoS_2 NGs with R_{Ex} was investigated (Fig. 4). As R_{Ex} increased, the output peak current (which is the maximum of $I(t)$ in the circuit, refer to t = 4 ns in Fig. 3(b)) decreased notably when R_{Ex} exceeded 10 MΩ, as shown in Fig. 4(a). The output peak voltage across the resistor became evident near R_{Ex} = 10 MΩ, and saturated near 100 GΩ, as shown in Fig. 4(b). Figure 4(c) shows the output peak power, which is the product of peak voltage and peak current. For the odd-layer NG in the present study, the output peak power reached the maximum value at R_{Ex} near 800 MΩ, and decreased as the number of layers increased. Figure 4(d) shows the energy conversion efficiency of the odd-layer NG, which was obtained as the electrical output energy of the NG divided by the mechanical deformation energy stored in the MoS_2 flake after being strained [13]. As the number of layers increased, the energy conversion efficiency exhibited a distinct decrease, which could be attributed to the higher mechanical deformation energy, larger C_{NG}, and lower V of the NG consisting of several MoS_2 layers. The above results indicate that single-layer NGs provide the largest piezoelectric output and highest energy conversion efficiency under the square-wave applied strain, and should be considered as preferential candidates in the fabrication of 2D NGs.

3.3 Output of MoS_2 NGs under high-frequency applied strain

Finally, in this section, the outputs of the MoS_2 NGs under high-frequency mechanical signals are analyzed. Figure 5(a) shows the $I_{sq}(t)$ values of a single-layer MoS_2 NG under a 5 GHz square-wave applied strain. Compared with the case of the 0.5 GHz applied strain, shown in Fig. 3(b), the peak current under a 5 GHz strain hardly relaxed in a half periodicity (0.1 ns) before the next peak current appeared, which caused a negative influence on the energy conversion efficiency.

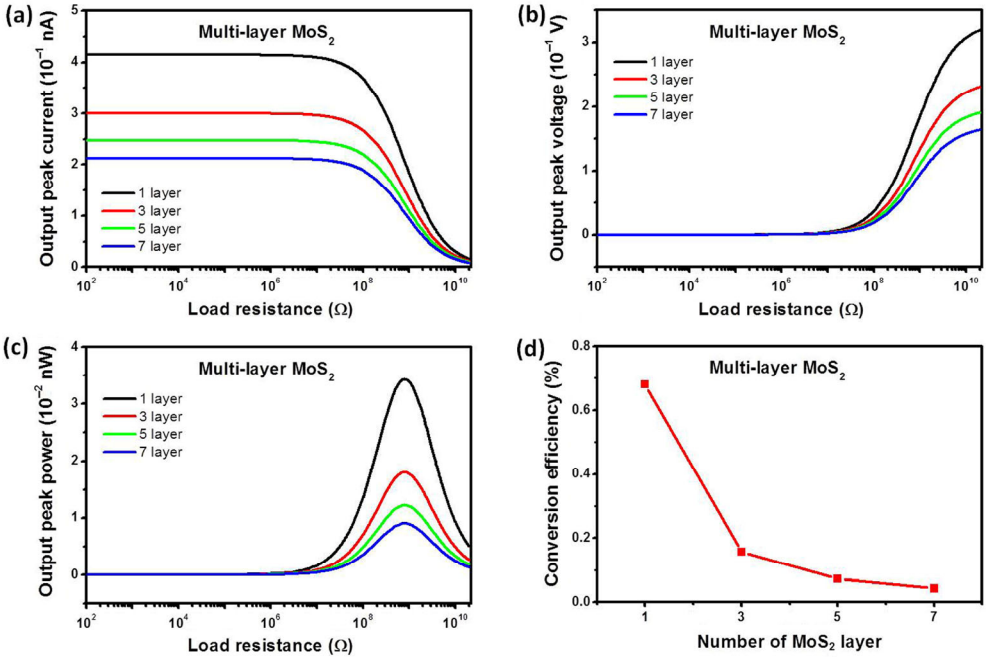

Figure 4 (a) Output peak current depending on the load resistance. (b) Output peak voltage across the resistor versus external resistance. (c) Output peak power on the load resistor as a function of the external resistance. (d) Energy conversion efficiency of NG versus layer number.

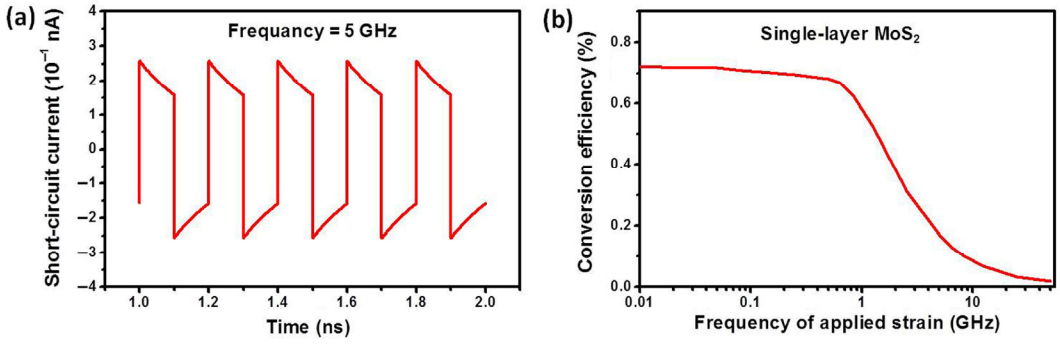

Figure 5 (a) Short-circuit current of single-layer MoS_2 NG under 5 GHz square-wave applied strain. (b) Energy conversion efficiency of single-layer MoS_2 NG versus frequency of the square-wave applied strain.

In Fig. 5(b), the energy conversion efficiency of the single-layer MoS_2 NG under different frequencies of the square-wave applied strain is shown. In the low-frequency region, the conversion efficiency almost retained a constant value. In contrast, in the high-frequency region, the conversion efficiency suffered an exponential decrease as the frequency increased, in agreement with the results of a previous study [24]. The decrease of the conversion efficiency was due to the lack of discharge time of the NG capacitor, as shown in Fig. 5(a). According to Fig. 5(b), the single-layer MoS_2 NG was capable of providing a satisfactory output until the signal exceeded 1 GHz, a value considerably higher than the frequency limit of the ZnO nanowire NG, which lies in the MHz region. We expect that the advantages of the MoS_2 NG working under high-frequency mechanical stimuli can be exploited in future experiments and device applications.

As indicated in the introduction section, MoS_2-based NGs have high tolerance to strain amplitude. Thus, in the present study, we also simulated the output characteristics of the MoS_2 NGs under large strain amplitude (up to 15%; other parameters, such as the MoS_2 flake size and NG R_{In}, were maintained identical to those used in the small-strain case); the results are shown in Figs. S1–S4 of ESM. Compared with the results of the small-strain case shown in Figs. 2–5, the MoS_2 NGs under large strain exhibited significantly higher output voltages and currents, showing a qualitatively similar dependence on the strain, flake length, and layer number to the small-strain case. On the other hand, the energy conversion efficiency hardly changed with the external mechanical strain, indicating the stable energy conversion by the MoS_2 NGs under an enormous applied strain. These results reveal the advantages of the MoS_2 NGs under large-strain conditions, which serve as guidance for the application of the next-generation 2D piezoelectric NGs.

4 Conclusions

We have investigated both the static and dynamical properties of MoS_2-based 2D NGs under external applied strains. Owing to the symmetrical restriction, only odd-layer MoS_2 NGs exhibited piezoelectric output. In addition, both the NG output current and energy conversion efficiency decreased as the number of MoS_2 layers increased. Furthermore, owing to the atomic-scale thickness, the C_{NG} of the MoS_2 NGs was at least an order of magnitude smaller than that of nanowire- and nanofilm-based NGs, which suggests the promising application of MoS_2 NGs under high-frequency mechanical signals. The present study provides not only a deeper understanding of the mechanism of 2D NGs, but also detailed guidance for their future design and optimization.

Acknowledgements

This work was supported by the "Thousands Talents" Program for Pioneer Researcher and his Innovation Team, China, and the National Natural Science Foundation of China (No. 51432005).

Electronic Supplementary Material: Supplementary material (Fig. S1 gives the static behaviors of the

MoS_2 NGs in case of large external applied strain; Fig. S2 gives the piezoelectric outputs of MoS_2 NGs without external load under a 15% external applied strain; Fig. S3 gives the piezoelectric outputs of odd-layer MoS_2 NGs under a square-wave external strain (15%) with an external load resistor; and Fig. S4 shows the piezoelectric outputs of the MoS_2 NGs under the high-frequency mechanical signal) is available in the online version of this article at http://dx.doi.org/10.1007/s12274-015-0959-8.

References

[1] Wang, Z. L.; Song, J. H. Piezoelectric nanogenerators based on zinc oxide nanowire arrays. *Science* **2006**, *312*, 242–246.

[2] Yang, R. S.; Qin, Y.; Dai, L. M.; Wang, Z. L. Power generation with laterally packaged piezoelectric fine wires. *Nat. Nanotechnol.* **2009**, *4*, 34–39.

[3] Kim, D. Y.; Lee, S.; Lin, Z.-H.; Choi, K. H.; Doo, S. G.; Chang, H.; Leem, J.-Y.; Wang, Z. L.; Kim, S.-O. High temperature processed ZnO nanorods using flexible and transparent mica substrates for dye-sensitized solar cells and piezoelectric nanogenerators. *Nano Energy* **2014**, *9*, 101–111.

[4] Lin, L.; Lai, C.-H.; Hu, Y. F.; Zhang, Y.; Wang, X.; Xu, C.; Snyder, R. L.; Chen, L.-J.; Wang, Z. L. High output nanogenerator based on assembly of GaN nanowires. *Nanotechnology* **2011**, *22*, 475401.

[5] Huang, C.-T.; Song, J. H.; Lee, W.-F.; Ding, Y.; Gao, Z. Y.; Hao, Y.; Chen, L.-J.; Wang, Z. L. GaN nanowire arrays for high-output nanogenerators. *J. Am. Chem. Soc.* **2010**, *132*, 4766–4771.

[6] Wang, C.-H.; Liao, W.-S.; Lin, Z.-H.; Ku, N.-J.; Li, Y.-C.; Chen, Y.-C.; Wang, Z.-L.; Liu, C.-P. Optimization of the output efficiency of GaN nanowire piezoelectric nanogenerators by tuning the free carrier concentration. *Adv. Energy Mater.* **2014**, *4*, DOI: 10.1002/aenm.201400392.

[7] Wang, X. B.; Song, J. H.; Zhang, F.; He, C. Y.; Hu, Z.; Wang, Z. L. Electricity generation based on one-dimensional group-III nitride nanomaterials. *Adv. Mater.* **2010**, *22*, 2155–2158.

[8] Huang, C.-T.; Song, J. H.; Tsai, C.-M.; Lee, W.-F.; Lien, D.-H.; Gao, Z. Y.; Hao, Y.; Chen, L.-J.; Wang, Z. L. Single-InN-nanowire nanogenerator with upto 1 V output voltage. *Adv. Mater.* **2010**, *22*, 4008–4013.

[9] Hu, Y. F.; Wang, Z. L. Recent progress in piezoelectric nanogenerators as a sustainable power source in self-powered systems and active sensors. *Nano Energy* **2015**, *14*, 3–14.

[10] Lee, K. Y.; Kumar, B.; Seo, J.-S.; Kim, K.-H.; Sohn, J. I.; Cha, S. N.; Choi, D.; Wang, Z. L.; Kim, S.-W. P-type polymer-hybridized high-performance piezoelectric nanogenerators. *Nano Lett.* **2012**, *12*, 1959–1964.

[11] Wang, Z. L. Self-powered nanosensors and nanosystems. *Adv. Mater.* **2012**, *24*, 280–285.

[12] Bai, S.; Zhang, L.; Xu, Q.; Zheng, Y. B.; Qin, Y.; Wang, Z. L. Two dimensional woven nanogenerator. *Nano Energy* **2013**, *2*, 749–753.

[13] Wu, W. Z.; Wang, L.; Li, Y. L.; Zhang, F.; Lin, L.; Niu, S. M.; Chenet, D.; Zhang, X.; Hao, Y. F.; Heinz, T. F. et al. Piezoelectricity of single-atomic-layer MoS_2 for energy conversion and piezotronics. *Nature* **2014**, *514*, 470–474.

[14] Bertolazzi, S.; Brivio, J.; Kis, A. Stretching and breaking of ultrathin MoS_2. *ACS Nano* **2011**, *5*, 9703–9709.

[15] Duerloo, K.-A. N.; Ong, M. T.; Reed, E. J. Intrinsic piezoelectricity in two-dimensional materials. *J. Phys. Chem. Lett.* **2012**, *3*, 2871–2876.

[16] Huang, X.; Li, L. J.; Zhang, Y. Modeling the open circuit output voltage of piezoelectric nanogenerator. *Sci. China Tech. Sci.* **2013**, *56*, 2622–2629.

[17] Bollinger, M. V.; Lauritsen, J. V.; Jacobsen, K. W.; Nørskov, J. K.; Helveg, S.; Besenbacher, F. One-dimensional metallic edge states in MoS_2. *Phys. Rev. Lett.* **2001**, *87*, 196803.

[18] Zhu, H. Y.; Wang, Y.; Xiao, J.; Liu, M.; Xiong, S. M.; Wong, Z. J.; Ye, Z. L.; Ye, Y.; Yin, X. B.; Zhang, X. Observation of piezoelectricity in free-standing monolayer MoS_2. *Nat. Nanotechnol.* **2015**, *10*, 151–155.

[19] Radisavljevic, B.; Radenovic, A.; Brivio, J.; Giacometti, V.; Kis, A. Single-layer MoS_2 transistors. *Nat. Nanotechnol.* **2011**, *6*, 147–150.

[20] Liu, W.; Zhang, A. H.; Zhang, Y.; Wang, Z. L. Density functional studies on edge-contacted single-layer MoS_2 piezotronic transistors. *Appl. Phys. Lett.* **2015**, *107*, 083105.

[21] Hu, Y. F.; Zhang, Y.; Xu, C.; Zhu, G.; Wang, Z. L. High-output nanogenerator by rational unipolar assembly of conical nanowires and its application for driving a small liquid crystal display. *Nano Lett.* **2010**, *10*, 5025–5031.

[22] Lu, C.-P.; Li, G. H.; Mao, J. H.; Wang, L.-M.; Andrei, E. Y. Bandgap, mid-gap states, and gating effects in MoS_2. *Nano Lett.* **2014**, *14*, 4628–4633.

[23] Zhou, J.; Gu, Y. D.; Fei, P.; Mai, W. J.; Gao, Y. F.; Yang, R. S.; Bao, G.; Wang, Z. L. Flexible piezotronic strain sensor. *Nano Lett.* **2008**, *8*, 3035–3040.

[24] Sun, C. L.; Shi, J.; Wang, X. D. Fundamental study of mechanical energy harvesting using piezoelectric nanostructures. *J. Appl. Phys.* **2010**, *108*, 034309.